

Polymerization Blending for Compatible Poly(ether sulfone)/Aramid Blend Based on Polycondensation of an *N*-Silylated Aromatic Diamine with an Aromatic Diacid Chloride in Poly(ether sulfone) Solution

HIDEO HAYASHI,¹ SHOICHI NAKATA,² MASA-AKI KAKIMOTO,² and YOSHIO IMAI^{2,*}

¹ Polymer Research Laboratory, Idemitsu Petrochemical Co., Ltd., Anegasaki-kaigan, Ichihara, Chiba 299-01, Japan;

² Department of Organic and Polymeric Materials, Tokyo Institute of Technology, Meguro-ku, Tokyo 152, Japan

SYNOPSIS

Poly(ether sulfone) (PES) and poly[*N,N'*-(oxydi-*p*-phenylene)isophthalamide] (44I) were blended readily by the polymerization-blending method; i.e., *N,N'*-bis(trimethylsilyl)-substituted bis(4-aminophenyl) ether was reacted with isophthaloyl chloride in the PES solution in DMAc, and the resulting mixture was directly cast into films. The procedure afforded transparent films over the entire PES/44I composition range. Homogeneous mixing of the component polymers in the form of films was shown by a single glass transition temperature, whereas a conventional solution-blending method afforded less compatible films in the PES-rich composition. This was also supported by morphological and infrared studies. The mechanical properties of the blend films, particularly the elongation-at-break, were improved by using the polymerization-blending method. © 1993 John Wiley & Sons, Inc.

INTRODUCTION

Aromatic poly(ether sulfone)s (PESs) such as poly(oxy-1,4-phenyleneisopropylidene-1,4-phenyleneoxy-1,4-phenylenesulfonyl-1,4-phenylene) (PSF)¹ and poly(oxy-1,4-phenylenesulfonyl-1,4-phenylene) (PES)² are well known as high-performance engineering thermoplastics. However, it is quite difficult to make one kind of PES possess all the characteristics and functions demanded. Polymer blends may exhibit a better balance of properties than each of the polymers alone. Hence, in recent years, a number of novel polymer blends based on PESs have been developed. For example, PSF-poly(*p*-phenylene sulfide) (PPS),³⁻⁷ PSF-poly(ether ketone) (PEK),^{8,9} PES-PPS,¹⁰ and PES-PEK¹¹⁻¹³ have been reported.

We recently reported that the binary blend of PES and aramid 44I, poly[*N,N'*-(oxydi-*p*-phenylene)isophthalamide], obtained through solution

blending at the composition of PES/aramid = 30/70 on a weight basis, gave a transparent compatible blend film despite being thermodynamically immiscible.¹⁴ Further, we found that the blend film showed an interesting crystallization behavior. Since PES is an amorphous polymer and the aramid is a dormant crystalline, the crystallization of the aramid was induced and accelerated dramatically at 300°C by blending PES, converting into a high-temperature resistant blend film.^{15,16}

It would be of great interest if we could achieve good compatibility of the binary blend over the whole PES/aramid composition ranges from the fundamental and technical viewpoints. One probable method to achieve this goal is "polymerization blending"; when the polycondensation forming polymer A is carried out in a solution of polymer B, the growing polymer chain of polymer A is mixed up in the solution so finely that the resulting solution composed of polymer A and polymer B is probably more compatible than is the corresponding solution obtained conventionally by solution blending of two solutions of the component polymers. A similar *in situ* direct polycondensation in the polymer matrix

* To whom correspondence should be addressed.

was reported by Ogata and his co-workers, who prepared opaque polyarylate films with finely dispersed rigid aramid or rigid polyarylate.¹⁷

We have developed a novel synthetic route, the *N*-silylated diamine method, for the synthesis of high molecular weight aramids starting from *N,N'*-bis(trimethylsilyl)-substituted aromatic diamines and aromatic dicarboxylic acid chlorides. The method is advantageous for the reasons that the polycondensation proceeds under neutral reaction conditions with the elimination of trimethylsilyl chloride and, hence, transparent flexible aramid films can be obtained directly by casting from the reaction solutions of the aramids just prepared. This method sounds suitable for the polymerization

blending of PES and aramid 44I and was extended successfully to the preparation of a compatible blend of the PES/aramid system by polymerization blending (Scheme 1).

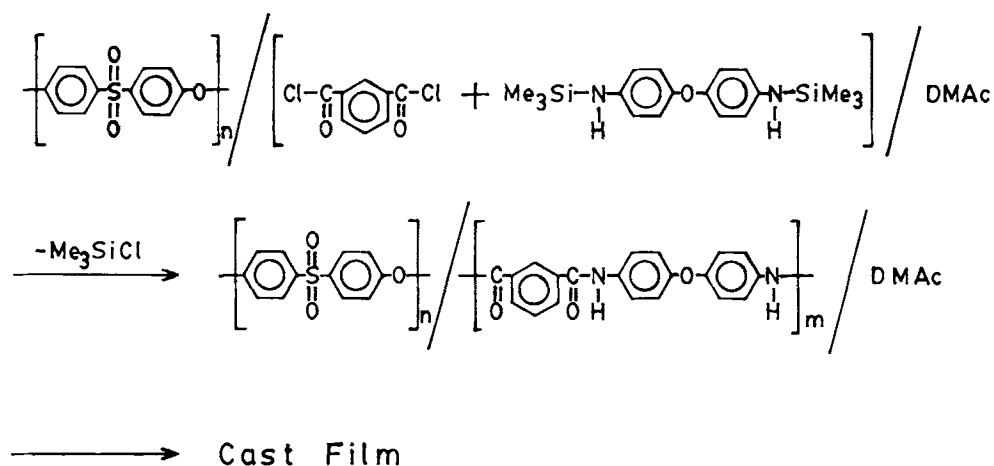
This article reports the compatibility, morphology, and properties of the polymerization-blended films of the PES/aramid system, including those of the solution-blended films for comparison.

EXPERIMENTAL

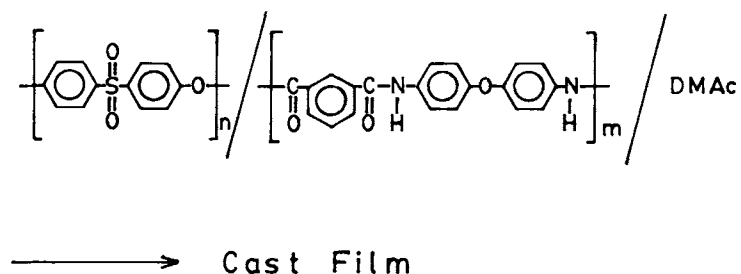
Materials

Aromatic poly(ether sulfone) (PES) was supplied by Imperial Chemical Industries, Ltd., as Victrex

Polymerization Blending



Solution Blending



Scheme 1

PES 300P, and used as received. Aramid 44I was prepared by a conventional method reported elsewhere.¹⁴ The inherent viscosities of PES and the aramid in *N*-methyl-2-pyrrolidone (NMP) at 30°C were 0.52 and 1.40 dL/g, respectively. *N,N'*-bis(trimethylsilyl)-substituted bis(4-aminophenyl) ether was synthesized according to the method reported previously.¹⁸ Isophthaloyl chloride was obtained commercially and purified by vacuum distillation. All the solvents such as NMP and *N,N*-dimethylacetamide (DMAc) were purified by distillation under reduced pressure.

Preparation of Polymerization-blended Films

A typical example of the preparation of the polymerization-blended film of the composition of PES/aramid = 30/70 on a weight basis is as follows: In a flask equipped with a mechanical stirrer, a nitrogen inlet, and a condenser with a drying tube, 0.707 g of PES was placed, and this was dissolved in 10 mL of DMAc with stirring under a slow stream of nitrogen. To the PES solution, 1.723 g (5.0 mmol) of *N,N'*-bis(trimethylsilyl)-substituted bis(4-aminophenyl) ether was added and dissolved completely. This solution was cooled with an ice-salt bath to -5°C. To the solution was added 1.015 g (5.0 mmol) of solid isophthaloyl chloride in one portion. The mixture was stirred at -5°C for 30 min and then at room temperature for 0–2.5 h under nitrogen. As the polycondensation proceeded, the solution became viscous, forming aramid 44I. The resulting polymer solution was cast onto a glass plate and dried under vacuum at room temperature for 24 h at 100°C for 24 h and at 220°C for 72 h, giving a transparent film of about 30 μm thick. The inherent viscosity of the aramid formed in the blend was estimated to be 1.2 dL/g, measured at a concentration of 0.5 g/dL in NMP at 30°C, by the extrapolation of the linear plot for the PES/aramid composition vs. the inherent viscosity of the blend to the intercept of the aramid. This relationship is based on the assumption that a plot of the PES/aramid composition vs. the inherent viscosity of the blend gives a straight line, because it was already confirmed in the case of the solution-blend system.

Preparation of Solution-blended Films

PES and the aramid were dissolved individually in DMAc at a concentration of 15 wt %. These two solutions were mixed and the combined solution was stirred at room temperature for 24 h for stabilization. The clear solution was cast onto a glass plate. Drying

conditions for the cast film were the same as those for the polymerization-blended film. The solution-blended films of about 30 μm were transparent or translucent in appearance, depending on the PES/aramid composition.

Measurement

Inherent viscosities of the polymers were measured at a concentration of 0.5 g/dL in NMP at 30°C with an Ostwald viscometer. Infrared spectra were recorded at room temperature on a JASCO FT/IR-5000 spectrophotometer. Weight-average molecular weight (M_w) and number-average molecular weight (M_n) were determined by gel permeation chromatography (GPC) on the basis of polyoxyethylene calibration on a JASCO apparatus (eluent: NMP). Differential scanning calorimetry (DSC) was performed with a Shimadzu thermal analyzer DSC-41M at a heating rate of 20°C/min in a nitrogen atmosphere. The midpoint of the slope change of the heat capacity plot of the DSC first scan was taken as the glass transition temperature (T_g). Dynamic mechanical analysis was performed with a Toyoseiki Reolograph-Solid at a frequency of 10 Hz and a heating rate of 2°C/min in air. Tensile properties were measured at room temperature using a Toyo Baldwin Tensilon UTM-II-20 with film specimens of 5 mm wide, 40 mm gauge length, and 30 μm thick. Five specimens for each sample were measured at a strain rate of 20%/min. The sample having the maximum elongation-at-break was taken as the data for elongation-at-break and tensile strength. The scanning electron micrographs were obtained with a JEOL JSM-25SIII scanning electron microscope (SEM) at an accelerating voltage of 15–30 kV. The sampling method for the observation of morphology with SEM was carried out as follows: The blend film was fractured at liquid nitrogen temperature, and the fracture surface was treated with chloroform at room temperature for 24 h to remove the PES domain. After that, the surface was coated with gold.

RESULTS AND DISCUSSION

Preparation of Polymerization-blended Films

The polycondensation of *N,N'*-bis(trimethylsilyl)-substituted bis(4-aminophenyl) ether with isophthaloyl chloride proceeded homogeneously in the PES solution in DMAc at room temperature over the entire PES/44I composition range. The inherent viscosities of aramid 44I formed were controlled in

Table I Inherent Viscosities of Aramid 44I Prepared by Polymerization Blending

η_{inh}^a (dL/g)	PES/44I Composition (wt/wt)				
	30/70	40/60	50/50	60/40	80/20
	1.2	1.3	1.3	1.3	1.2

* Measured at a concentration of 0.5 g/dL in NMP at 30°C.

the range of 1.1–1.3 dL/g, as shown Table I, since the molecular weight can affect the compatibility of the binary polymer blend. Figure 1 shows the infrared spectra of the PES/44I blend film by polymerization blending and the component polymer films. The appearance of a peak at 1650 cm^{-1} (amide I absorption) confirmed the formation of aramid 44I in the PES solution. Figure 2 shows the GPC curves of PES and the PES/44I blend by polymerization

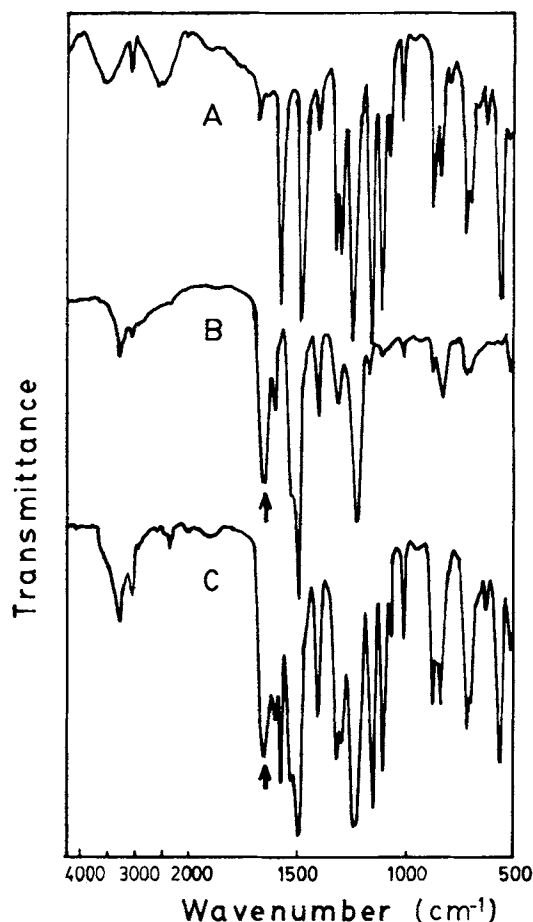


Figure 1 Infrared spectra of the polymer films: (A) PES; (B) aramid 44I; (C) PES/44I 50/50 blend by polymerization blending.

blending. Since the curve of the aramid with an inherent viscosity of 1.1–1.3 in the polymerization blend overlaps with that of PES, the aramid of high molecular weight ($\eta_{inh} = 4.0$ dL/g) in the polymerization blend was used for the GPC study. Although PES showed a bimodal curve, these two curves were very similar in shape with respect to PES component. The \bar{M}_n , \bar{M}_w , and \bar{M}_w/\bar{M}_n values of PES and those of PES in the polymerization blend were calculated to be 19,000, 41,000, and 2.2, and 19,000, 43,000, and 2.3, respectively. Thus, the \bar{M}_n , \bar{M}_w , and \bar{M}_w/\bar{M}_n values of neat PES agreed quite well with those of PES in the polymerization blend. In other words, the \bar{M}_n , \bar{M}_w , and \bar{M}_w/\bar{M}_n values of PES did not change throughout the polymerization blending and, therefore, no reaction such as chain extension had occurred on PES during the polymerization.

Compatibility of Polymerization Blends

Polymerization blending gave transparent PES/44I films over the entire composition range. In contrast, conventional solution blending gave the translucent phase-separated PES/44I films at the PES-rich composition. Figure 3 shows the DSC thermograms of the first runs of the polymerization blends and those of the solution blends with the PES/44I 50/50 composition. As shown in this figure, the polymerization blends exhibited a single T_g , whereas the solution blends exhibited two T_g 's. Figure 4 shows

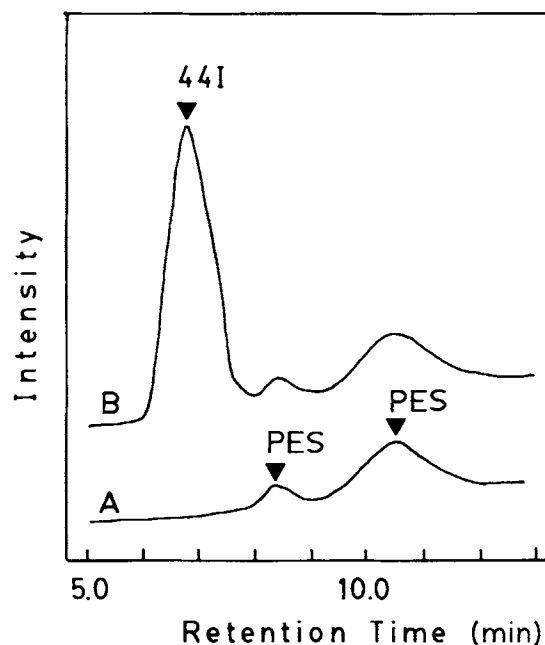


Figure 2 GPC curves of the polymers: (A) PES; (B) PES/44I 30/70 by polymerization blending.

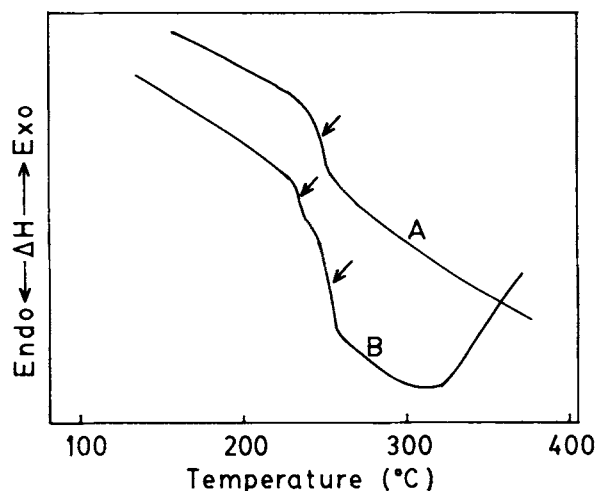


Figure 3 DSC thermograms of the first runs for the blend films: (A) 50/50 PES/44I polymerization blend; (B) 50/50 solution blend.

the T_g of the polymerization blends and those of the solution blends. The polymerization blends exhibited apparently a single T_g over the entire composition range and the T_g was at a temperature between those of the individual constituent polymers (225°C for PES and 270°C for aramid 44I). The single

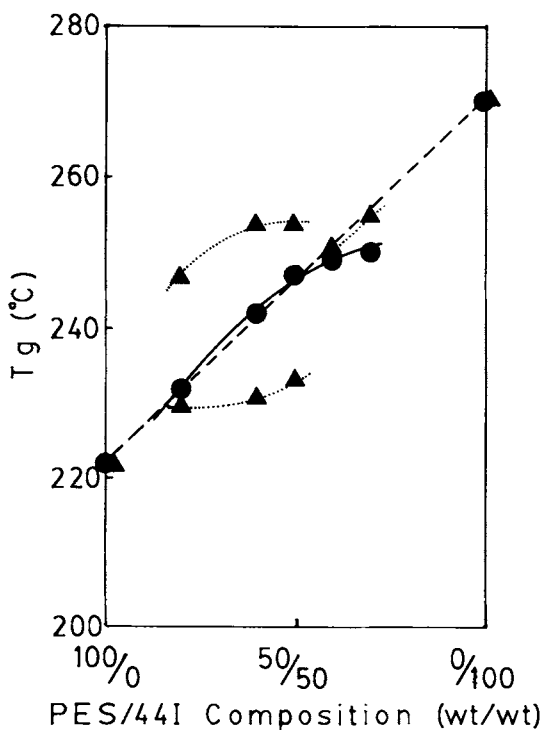


Figure 4 Composition dependence of T_g for the blends: (●) polymerization blend; (▲) solution blend. Dashed line represents calculated T_g values based on linear mixture rule.

composition-dependent T_g 's suggest good compatibility in the binary PES/44I polymerization blends. This corresponded well to the fact that transparent films formed from the polymerization blends mentioned above. In addition, the intermediate T_g of the compatible polymerization blends lies close to that predicted by an interpolation of the T_g 's of the blend constituents based on the linear mixture rule:

$$T_g = W_1 T_{g1} + W_2 T_{g2}$$

where T_{g_i} and W_i are the T_g and the weight fraction of the i -th component, respectively. In the case of the PES/44I solution blends, though the 40/60 and 30/70 blends exhibited a single T_g , the others displayed two T_g 's corresponding to the composition of each phase, indicative of phase-separated blends giving translucent films.

The compatibility of the PES/44I blends at the molecular level was studied by IR spectroscopy. Figure 5 shows the composition dependence of the absorption maximum in the N—H stretching band of the polymerization blends and the solution blends. It is apparent, and has been already reported,¹⁶ that a shift of the peak position toward higher wavenumbers from 3304 cm^{-1} in pure 44I is brought about by blending with PES. Since the dissociation of the

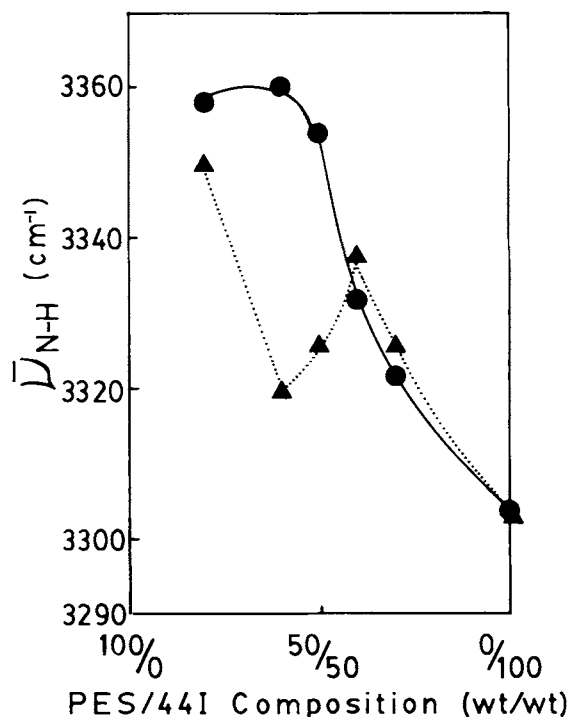
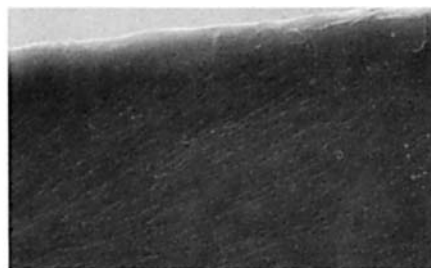


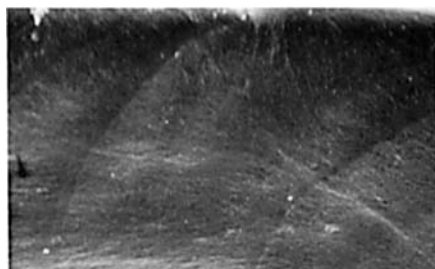
Figure 5 Composition dependence of wavenumber of N—H absorption peak for the blend films: (●) polymerization blend; (▲) solution blend.



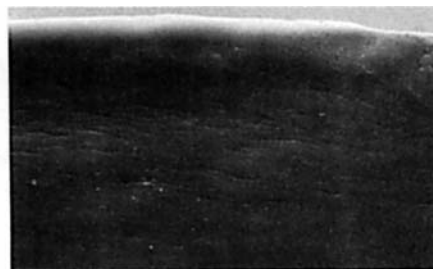
30/70



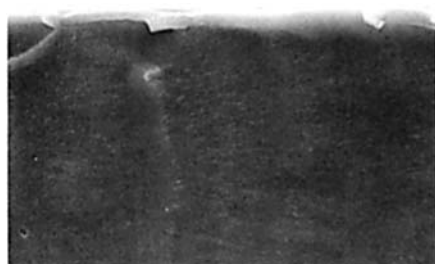
30/70



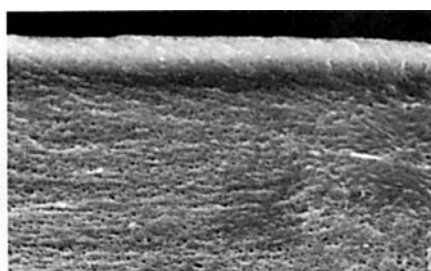
40/60



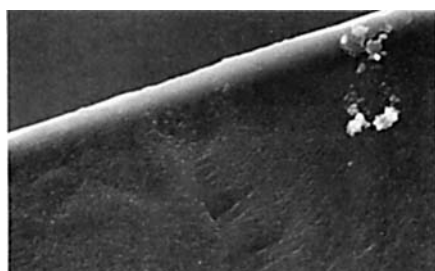
40/60



50/50

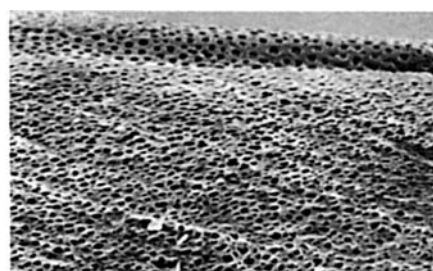


50/50



10 μ m

PES/44I=60/40



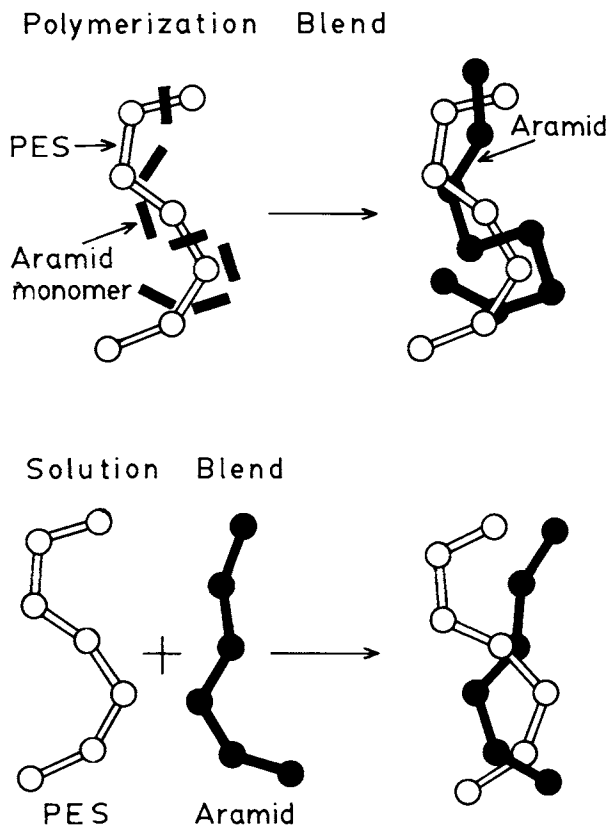
10 μ m

60/40

Polymerization Blended Films

Solution Blended Films

Figure 6 SEM micrographs of fractured surface of polymerization-blended films and solution-blended films.



Scheme 2

hydrogen bonding between amide–amide groups is caused by dilution of the aramid molecules through blending with PES, the larger value of the upfield shift implies the existence of intermolecular hydrogen bonding between the aramid and PES and, hence, better compatibility of the blends.

In more detail, the maximum peaks of the N—H stretching band are shifted about 50 cm^{-1} from 3304 to 3360 cm^{-1} in the polymerization blends with the composition between 0/100 and 60/40, where a plateau value is reached. In the case of the solution-blend system, the composition dependence of the absorption maximum is rather complicated. The wavenumbers of the N—H absorption of the solution blends with the composition of 50/50 and 60/40 were far lower than those of the corresponding polymerization blends, whereas the rest of the solution blends almost followed the line for the polymerization blends. This suggests that the solution blends with 50/50 and 60/40 compositions have lower compatibility at the molecular level compared with the polymerization blends.

Figure 6 shows SEM micrographs of the polymerization-blended films and the solution-blended films. All the films of the polymerization blends with PES/aramid 30/70, 40/60, and 60/40 compositions were homogeneous and did not show any phase-separation structure. These results imply that PES in

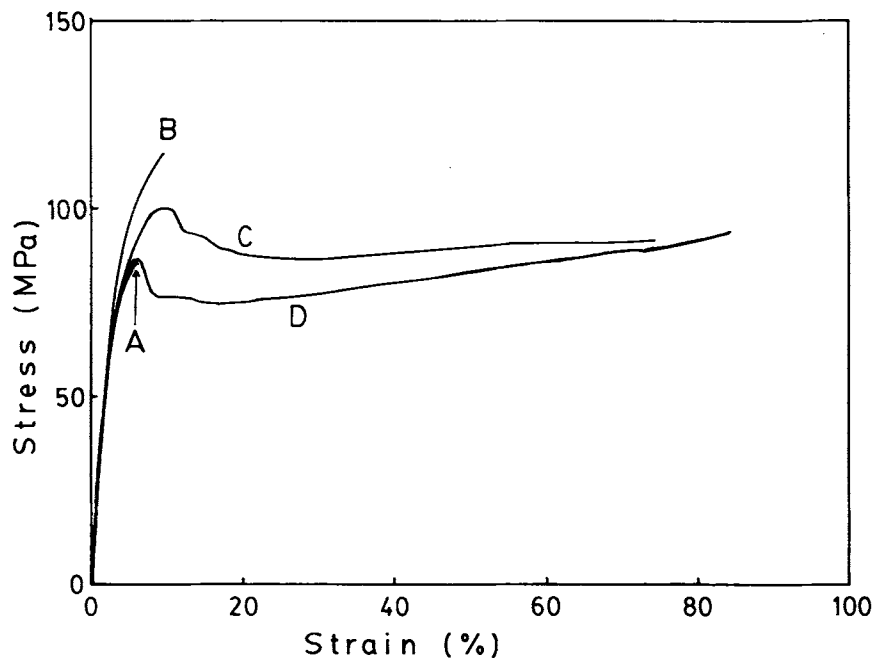


Figure 7 Stress–strain curves for the films of (A) PES, (B) 44I, (C) 50/50 PES/44I polymerization blend, and (D) 50/50 solution blend.

the polymerization blends could not be removed by treating with chloroform because of good compatibility. This corresponds well to the fact that these films were all transparent. In the case of the solution-blended films, the blends with aramid-rich compositions of 30/70 and 40/60 were homogeneous, whereas those having 50/50 and 60/40 compositions were two-phase structures with the PES domain dispersed in the aramid matrix. The diameter of the PES domain for the 60/40 blend was found to be 0.2–0.5 μm and was larger than that of the 50/50 blend having less than 0.1 μm . In fact, the phase separation led to translucent films in these blends.

From these results, it was found that the compatibility of the binary mixture of PES and the aramid was greatly improved by polymerization blending. This is probably because the growing aramid molecules are interpenetrated in the PES molecules in solution, resulting in the formation of a highly entangled mixture of PES and the aramid as

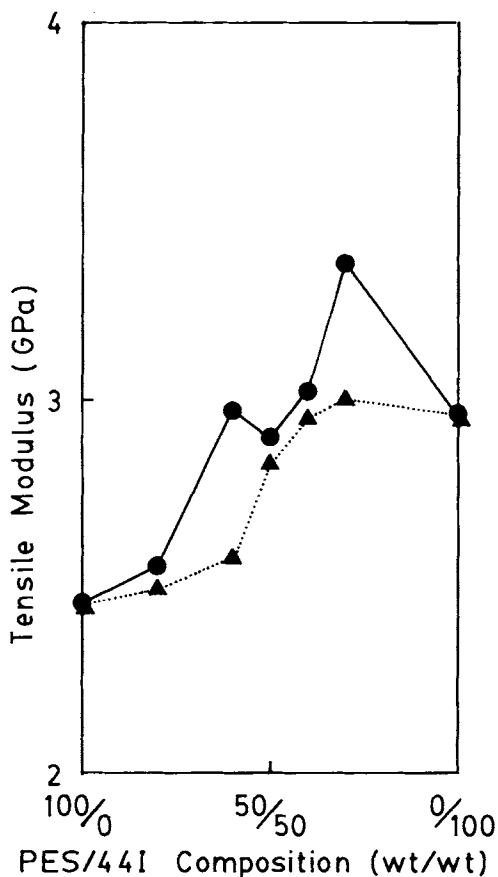


Figure 8 Composition dependence of tensile modulus for the blend films: (●) polymerization blend; (▲) solution blend.

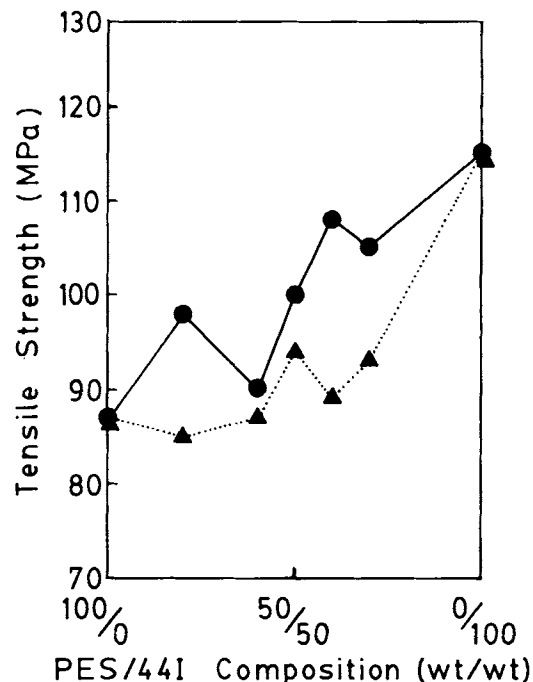


Figure 9 Composition dependence of tensile strength for the blend films: (●) polymerization blend; (▲) the solution blend.

shown in Scheme 2, and, hence, the mixture solution is very difficult to phase separate into the component polymers during casting films. However, in the case of the solution blends, the degree of entanglement of the aramid and PES is lower than that of the polymerization blends, as shown in Scheme 2.

Mechanical Properties of the Polymerization-blended Films

Figure 7 shows the stress–strain curves for the films of PES, the aramid, the PES/aramid 50/50 polymerization blend, and the 50/50 solution blend. A comparison of the curves showed a significant increase in elongation-at-break of both polymerization-blended film and solution-blended film, regardless of the blending method. The composition dependence of tensile modulus, tensile strength, and elongation-at-break for both polymerization-blended films and solution-blended films are shown in Figures 8, 9, and 10, respectively. The tensile modulus and tensile strength of the polymerization-blended films were slightly higher than those of the solution-blended films. The polymerization-blended films had the characteristic of high elongation-at-break, and, especially, the blends yielded the films having elongation over 50% in relatively wide com-

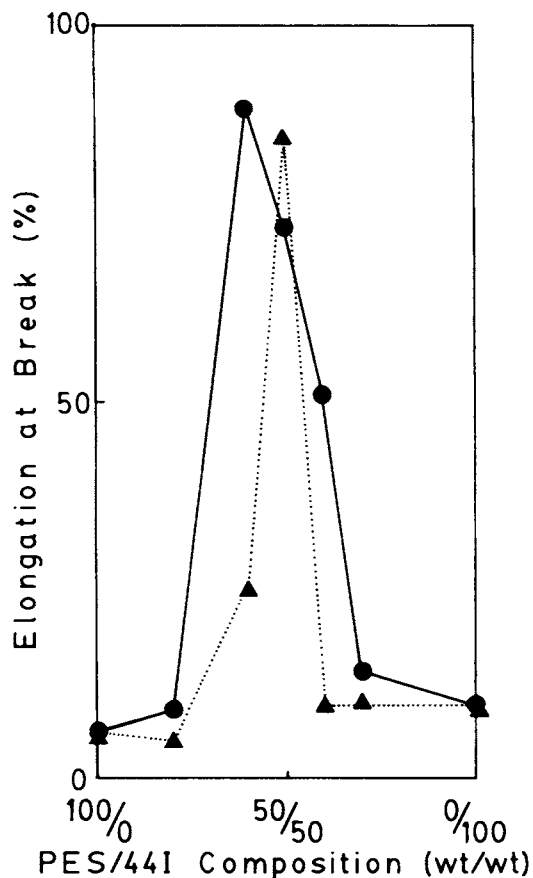


Figure 10 Composition dependence of elongation-at-break for the blend films: (●) polymerization blend; (▲) solution blend.

position ranges of PES/aramid of 40/60 to 60/40. This may be explained as follows: The elongation-at-break of neat PES film cast from DMAc solution was only 6%, whereas that of the commercial extrusion-molded film is 226% (Sumitomo Chemical Co.). The former is because DMAc is a poor solvent for PES and because the macromolecular chain of PES in the solvent has a collapsed structure, which is retained due to the relatively high evaporation speed of DMAc during casting the film, and, hence, the degree of entanglement of the PES chain is relatively low. The compatible PES/aramid films with the composition of near 50/50 obtained by polymerization blending probably have a mutually entangled structure of the aramid and PES due to good compatibility at the molecular level, and, therefore, high elongation results from the entanglement. In case of solution blending, only the film with the 50/50 composition having phase-separated morphology had exceptionally high elongation; however, the reason is unclear yet.

CONCLUSION

It was found that the compatibility of the binary mixture of PES and aramid 441 was greatly improved by the polymerization-blending method. Polymerization blending gave the films better tensile properties than did solution blending, especially high elongation-at-break (50–90%) over relatively wide PES/aramid composition ranges. Therefore, this method is advantageous over solution blending and widely applicable to improve the compatibility of many immiscible blend systems and also tensile properties of blend films.

REFERENCES

1. R. N. Johnson, A. G. Farnham, R. A. Cledinning, W. F. Hale, and C. N. Merriam, *J. Polym. Sci. Part A-1*, **5**, 2375 (1967).
2. T. E. Attwood, D. A. Barr, T. King, A. B. Newton, and J. B. Rose, *Polymer*, **18**, 359 (1977).
3. H. Zeng and K. Mai, *Makromol. Chem.*, **187**, 1787 (1986).
4. M.-F. Cheung, A. Golovoy, H. K. Plummer, and H. Vanoene, *Polymer*, **31**, 2299 (1990).
5. M.-F. Cheung, A. Golovoy, and H. Vanoene, *Polymer*, **31**, 2307 (1990).
6. M.-F. Cheung and H. K. Plummer, *Polym. Bull.*, **26**, 349 (1991).
7. S. Akhtar and J. L. White, *Polym. Eng. Sci.*, **31**, 84 (1991).
8. Q. Guo, J. Huang, and T. Chen, *Polym. Bull.*, **20**, 517 (1988).
9. Q. Guo, J. Huang, T. Chen, H. Zhang, Y. Yang, C. Hou, and Z. Feng, *Polym. Eng. Sci.*, **30**, 44 (1990).
10. X. Zhang and Y. Wang, *Polymer*, **30**, 1867 (1989).
11. C. K. Sham, C. H. Lau, D. J. Williams, F. E. Karasz, and W. J. MacKnight, *Br. Polym. J.*, **20**, 149 (1988).
12. Z. Wu, Y. Zheng, X. Yu, T. Nakamura, and R. Yosomiya, *Angew. Makromol. Chem.*, **171**, 119 (1989).
13. Z. Wu, Y. Zheng, H. Yan, T. Nakamura, T. Nozawa, and R. Yosomiya, *Angew. Makromol. Chem.*, **173**, 163 (1989).
14. S. Nakata, M. Kakimoto, and Y. Imai, *Polym. J.*, **20**, 80 (1990).
15. M. Matsuura, H. Saito, S. Nakata, Y. Imai, and T. Inoue, *Polymer*, **33**, 3210 (1992).
16. S. Nakata, M. Kakimoto, and Y. Imai, *Polymer*, **33**, 3873 (1992).
17. N. Ogata, K. Sanui, and H. Itaya, *Polym. J.*, **22**, 85 (1990).
18. Y. Oishi, M. Kakimoto, and Y. Imai, *Macromolecules*, **21**, 547 (1988).

Received June 17, 1992

Accepted December 15, 1992